IEEE Access
Multidisciplinary | Rapid Review | Open Access Journal

Date of publication xxxx 00, 0000, date of current version xxxx 00, 0000.

Digital Object Identifier 10.1109/ACCESS.2017.DOI

Projection-based collision detection algorithm for stereoelectroencephalography electrode risk assessment and re-planning

ALFREDO HIGUERAS-ESTEBAN[1,2], IGNACIO DELGADO-MARTÍNEZ[1], LAURA SERRANO[3], NAZARET INFANTE-SANTOS[3], ALEJANDRA NARVÁEZ-MARTÍNEZ[3], ALESSANDRO PRINCIPE[4], RODRIGO ROCAMORA[4], GERARDO CONESA[3], LUIS SERRA[1], and MIGUEL A. GONZÁLEZ BALLESTER[2,5],

[1]Galgo Medical SL, Neurosurgery Unit, Barcelona, Spain (e-mail: info@galgomedical.com)
[2]Universitat Pompeu Fabra, BCN Medtech, Dept. of Information and Communication Technologies, Barcelona, Spain
[3]IMIM-Hospital del Mar, Neurosurgery, Barcelona, Spain
[4]IMIM-Hospital del Mar, Epilepsy Unit, Barcelona, Spain
[5]ICREA, Barcelona, Spain

Corresponding author: Alfredo Higueras-Esteban (e-mail: alfredo.higueras@galgomedical.com).

This work was supported in part by Fundació "la Caixa" (Barcelona, Spain) with a Convenio Generalitat grant.

ABSTRACT Surgical planning is crucial to Stereoelectroencephalography (SEEG), a minimally invasive procedure that requires clinicians to operate with no direct view of the brain. Decisions making involves different clinical specialties and requires analysis of multiple multimodal datasets. We present a DepthMap tool designed to localize, measure, and visualize surgical risk, and an AlternativeFinder tool, designed to search for alternative trajectories maintaining adherence to the initial trajectory with three different re-planning strategies: similar entry, similar target, or parallel trajectory. The two tools transform the 3D problem into the 2D domain using projective geometry and distance mapping. Both use the graphics processing unit (GPU) to create a 2D depth image used by DepthMap for measurement and visualization, and by AlternativeFinder to find alternative trajectories. Tools were tested with 12 SEEG cases using digital subtraction angiography. DepthMap was used to measure vessel distance. AlternativeFinder was then used to search for alternatives. Computation time and displacements of the entry and target points for each trajectory and adherence strategy were recorded. The DepthMap tool found vessels in 118 initial trajectories (out of 145). Ninety alternative trajectories were found to meet the required avascular constraints (average 820K alternatives evaluated per initial trajectory). The average computation time was 449 ms per initial trajectory (77 ms when alternatives were found). The tools presented helped clinicians examine and re-plan SEEG trajectories to avoid vascular risks using three adherence strategies. Quantitative measurement of the adherence shows the potential of this tool for clinical use.

INDEX TERMS Biomedical informatics, DICOM, Depth electrodes, Epilepsy, Implants, Path planning, Stereoelectroencephalography (SEEG), Stereotactic surgery, Surgery planning

I. INTRODUCTION

AROUND one-third of epileptic patients do not respond to antiepileptic drugs [1] and could be treated with epilepsy surgery [2]. Stereoelectroencephalography (SEEG) is a stereotactic technique used in complex drug-resistant epilepsy cases to evaluate a possible surgical intervention [3]–[6]. This is an invasive technique that consists of the placement of several rectilinear depth electrodes. It is used to measure electric fields inside the brain with the multiple contacts in a row placed in each trajectory [7].

SEEG is an invasive technique that is performed on selected patients to answer clinical questions when a clear chance for a surgical solution is feasible, and previous non-invasive information is not enough to elucidate proposed

options for depicting the epileptogenic zone (EZ) and epileptic network. This noninvasive patient information includes seizure semiology, especially the initial symptoms that appear at seizure start, neuropsychology testing, MRI, video EEG recordings, and frequently PET scanning and ictal and interictal (and SISCOM) information. It may be difficult to understand the onset area from video-EEG surface electrodes recordings (mostly when it is deep as for instance if it originates from the insula, the orbital frontal, the mesial structures as the cingulum), or to elucidate the side of seizure onset in a rapidly generalizing seizure.

The implantation of SEEG requires careful planning of the trajectories. The SEEG trajectory plans evolve from an initial draft which evolves in successive degrees of refinement until a final surgical plan is obtained. SEEG has a strong multidisciplinary component [8], [9], with epileptology and neurosurgery being the most involved clinical specialties. In this document, we use the term initial plan to denote a concept similar to the 'epileptologist plan' [10], [11] or 'the strategy of the implantation' [12], [13] mentioned in related literature.

The initial steps of the SEEG workflow that is carried out at Hospital del Mar, Barcelona requires the epileptologists to suggest an initial trajectory plan based on an EZ localization hypothesis based on non-invasive clinical information. Following that initial plan from the epileptologist, neurosurgeons modify the initial plan looking for safe trajectories, taking into account the new information incorporated about cerebral vascularization (e.g., DSA or CT scans) and adapt that plan for surgical safety [10]. The work presented here starts right after the epileptologist has provided its initial trajectories, and it is aimed at aiding neurosurgeons with tools to early detect and discard high-risk trajectories and find alternative ones when required.

There is consensus that the most important risk to avoid is intracranial bleeding [3], [6], [14] which can cause significant damage or death. Special attention is taken to avoiding vessels at the beginning of the trajectory in the cortex, as they are associated with greater bleeding risk [11]. Surgical planning is patient-dependent and has been described as a time-consuming and inefficient process [15]. It may involve the visual inspection of multiple 2D slices from 3D imaging datasets so that a cylinder shape that surrounds the electrode, commonly referred to as the security zone (SZ) is free of vascular structures to be avoided. During the rest of the manuscript, the SZ is defined by the diameter of the cylinder that has the trajectory as its main axis. The SZ used depends on the precision of the implantation device (e.g., surgical robot) and institution/clinician criteria.

Previous work in stereotactic automatic planning has been presented for Deep Brain Stimulation (DBS) [16], needle biopsy [17], [18], SEEG [19], [20] and other straight-access neurosurgical interventions [21], [22]. For procedures where only the tip is active (e.g., DBS, needle biopsy, or laser ablation) a common approach is to compute the optimal entry point given the desired target defined by the user. However, this strategy is not entirely sufficient for SEEG electrodes, which measure electrical data along its entire length.

Specifically for SEEG planning, the Milan group presented a method that takes into account the distance from vessels, sulci avoidance, and penetration angle based on the user selection of one target point and an entry region [19]. The method was later modified so that the user selects a rough entry and a rough target [23]. This work was further developed to optimize trajectories [11] computing for each trajectory all possible entry-target combinations from within a user-defined entry and target permitted areas, where the exact number of candidate entry and target points was defined by image resolution. In its evaluation study clinicians were asked to rank qualitatively (either 'good', 'acceptable' or 'discarded') the adherence of the alternative trajectory to the initial one, both at the entry and the target regions. In a later work from the same group, a new method was presented with an increased computational speed of 160±102 s/trajectory [15]. To increase safety, a Maximum Intensity Projection (MIP) method was presented which takes into consideration the first centimeter of the trajectory [24].

Epinav™ is another software platform for automated SEEG planning, reaching interactive rates for finding alternative entry points for a given target point. Then a method is presented which is dependent on the skull mesh segmentation results to initialize the search [20]. More importantly, the method searches for the best entry point for a given target but cannot be used to search for the best target point for a desired entry. It makes fast computations using the GPU (5000 candidate entry points in 250ms). Epinav™ also has a visualization tool that provides a graph for each trajectory in which the horizontal axis represents the length of the electrode, and the vertical one represents the distance to the nearest critical structure in any direction. Later in [25], a multiple trajectory planning algorithm was presented which, takes into consideration the amount of gray matter traversed to increase electrode efficacy, apart from considering electrode collisions. The reported time was below a minute for 7-12 electrode plans. Regarding alternative path computations, results are displayed with a color-coding directly on the skull surface, similarly to other tools published for DBS [26], needle biopsy [17], [18], and general keyhole neurological interventions [21], [27]–[29].

Zelmann *et al.* [30] presented another method that also considers the location of individual contacts to maximize recording volume while constraining the trajectories to safe paths, considering a wide variety of constraints. Only 3 target structures per hemisphere were considered (1 in the amygdala and 2 in the hippocampus) and a distance map is computed from the surface inwards to represent the greater importance of measuring from the center of the structure. Gaussian sampling was used to sample possible target points from segmented deep target structures and possible entry points from the entry regions to favor the evaluation of trajectories traversing central areas. On average, 7 minutes per optimized trajectory was reported.

This article has been accepted for publication in a future issue of this journal, but has not been fully edited. Content may change prior to final publication. Citation information: DOI 10.1109/ACCESS.2021.3099964, IEEE Access

Most of the described approaches focus on adhering to the distal target (e.g., hippocampus). However, the proximal entry point of the brain is sometimes critical in SEEG. This entry point may be crucial to measure from an identified structural lesion (e.g., abnormal brain tissue) or a superficial functional cortical region such as Broca's or Wernicke's [9], [31]. Although adherence to the entry or the target has been used for qualitative alternative evaluation, but to the best of our knowledge it has not been used as an input to the optimization. Furthermore, adherence to the insertion angle is yet another form of adherence that might be useful for SEEG approaches (such as [32]) in which all trajectories are as parallel as possible to each other. Thus, there is a need for an automated trajectory planning tool that takes as input different approaches to maintain adherence to the initial plan, and which performs at interactive rates.

II. METHOD

In this section, the two tools used by our method, the DepthMap and the AlternativeFinder, will be described, as well as their integration with a GUI and its experimental evaluation. A combination of projective geometry and distance map computation is used to transform the 3D problem into the 2D domain to simplify the problem and speed up computation. The tools will be presented to avoid volumetric no-go zones (i.e., vessels) which we will refer to as the mask volume. This mask volume is obtained by registering and merging all DSA datasets into one and then performing a threshold segmentation. Those DSA datasets contain venous and arterial information of each patient (two for each implanted brain hemisphere). Nevertheless, the described functionality can be used with other datasets and can be adapted to consider go zones and/or mesh inputs. The description also assumes that the datasets are contained in a scene graph data structure and are registered via relative transformations [33], [34].

A. DEPTHMAP TOOL

The DepthMap tool accepts two inputs: a mask volume containing no-go zones and a trajectory. The tool is designed to early detect and visualize critical structures within the SZ of the trajectory. It works by projecting the portion of the mask volume contained inside the trajectory SZ into 2D space to create a depth image, which contains depth information for each rendered pixel. Later, that depth image is evaluated to find 'cylindrical SZ vs. no-go zone' collisions. This procedure shares similarities with the MIP implementation presented in [24]. A preliminary version of this tool was presented in [35] and mentioned in [34].

To obtain the depth image, a rendering pipeline needs to be configured. First, a mask volume is positioned in object space with a transformation parametrized by several DICOM tags (e.g., pixel spacing, image orientation). Then, it is multiplied by its model transform T_{model}, obtained by concatenating all its ancestor relative transformations contained in the scene-graph, which again modifies its pose (i.e., translation and orientation) placing it in world space (i.e., registered). The view transform T_{view} is then applied, leaving data in camera space, which is centered at the entry point facing the target point. The next step is to apply an orthographic projection T_{proj} defined by the smallest square prism which fits the cylindrical security zone of the trajectory (Fig. 1). After that perspective division takes place, and finally, the viewport transform $T_{viewport}$ maps the result to the final 2D image (resolution of 128×128 pixels).

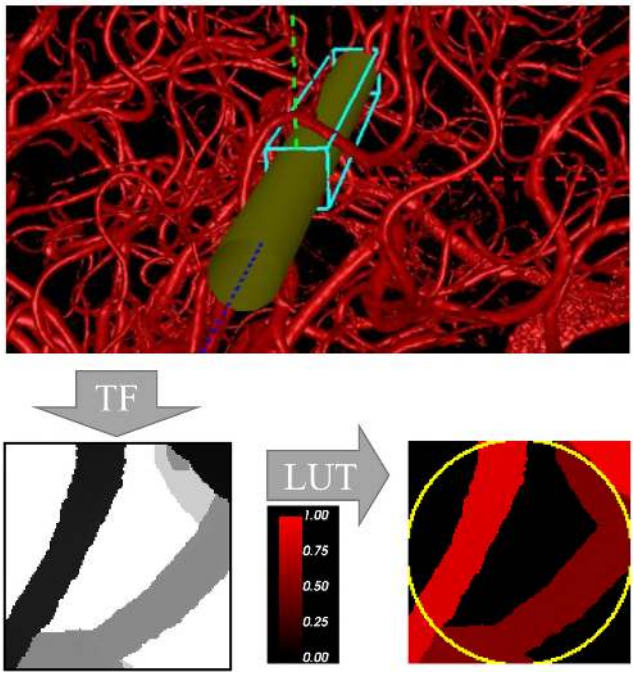

FIGURE 1. Volume rendering of one of the angiographies (i.e., vessel mask volume) depicting a cylindrical security zone in yellow and an orthographic frustum in cyan (top). Depth image in black and white (bottom left) and final image used in GUI (bottom right), both with a non-linear color mapping to enhance visualization. The 3D cylindrical security zone is prolonged towards the outside of the head for clinical visualization purposes.

After the rendering, the depth image (i.e., z-buffer) is retrieved. A non-linear look-up-table (LUT) is used to map each value of the depth image from black (far clipping plane) to a solid color (near clipping plane). The pixels inside the circumference that are not black (i.e., depth different than the far clipping plane) represent vessels inside the SZ. The algorithm takes advantage of the volume rendering capabilities provided by VTK [36].

An approximate formulation of the order in which each step is applied can be represented by the following equation:

$$DepthMap_{2D} = T_{viewport} \cdot PerspectiveDivide(T_{proj} \cdot T_{view} \cdot T_{model} \cdot Image_{3D}) \quad (1)$$

Radial distance to critical structures is preserved under the orthographic projection, allowing for the computation of the distance from closest vessel to electrode axis by measuring the closest non-null pixel to the 2D depth image center. The span of the trajectory can be subdivided (e.g., entry region

This article has been accepted for publication in a future issue of this journal, but has not been fully edited. Content may change prior to final publication. Citation information: DOI 10.1109/ACCESS.2021.3099964, IEEE Access

and rest), allowing for the computation of vascular distances on each subpart of the trajectory. Please note that in this tool and the rest of the manuscript, distance to vessels is expressed in diameter, instead of radius, to comply with the SZ definition used in some robotic implantation systems.

B. ALTERNATIVEFINDER TOOL

This tool also takes as input a mask volume containing no-go zones and a trajectory. Its purpose is to find alternative trajectories (i.e., trajectories without vessels inside the SZ) that adhere to a given initial trajectory. The metric to decide what is closer (or more adherent) is selected by the user from among three available options: trajectories with similar entry, similar target, or parallel (with the same angle relative to world coordinates).

In contrast with the DepthMap tool, where each depth image computation allowed for the computation of one trajectory, the Trajectory Finder computes for each render as many trajectories as pixels contained in the 2D depth image (currently 128×128 pixels, resulting in over 16K alternatives/depth image).

First, the Signed Mauer distance map algorithm [37] is used to create a distance map from the binary image. A transfer function is created and configured with a Boolean predicate function, mapping 1 (fully opaque) to values smaller than the SZ radius of the trajectory, and 0 (transparent) to those above it. When visualizing the distance map with that transfer function, a fattened version of the vessel tree appears. The reason to perform this operation is that finding vessels inside the security zone (this time defined by a capsule instead of a cylinder) is equivalent to finding the intersection between line segments and the threshold distance map described (Fig. 2).

The parametrization of the rendering is the same as in the DepthMap tool, apart from the location of the camera, and the use of orthographic (parallel) or perspective (similar entry/target) projection (Fig. 3), which depends on the adherence strategy selected:

- *Similar entry*: a perspective camera located at the entry point facing towards the target point. Field-of-view is set to 15°.
- *Similar target*: same as the previous one but located at the target point facing the entry point.
- *Parallel*: same parameters as in the previously described step. Resolution and lateral frustum bounds could be modified to affect trajectory density and search space.

After the rendering, depth is recovered, where each pixel with a value of 0 represents an avascular trajectory with no vessels inside its SZ, (P2 in Fig. 4). Then, the closest 0-value-pixel from the image center (P1 in Fig. 4), if found, is used to compute its associated trajectory. For that, all pose transformations described for the DepthMap tool must be applied to P2 in reverse order.

In the similar entry strategy, when an alternative is not found in the first render, the search continues moving the entry (P0), spiraling away on each iteration (n) in a plane perpendicular to the trajectory, following a pattern (Fig. 5) described by (2) were radial distance RD is 0.1 mm and ω is $\approx 135.5°$, an approximation of the golden ratio in the angular form.

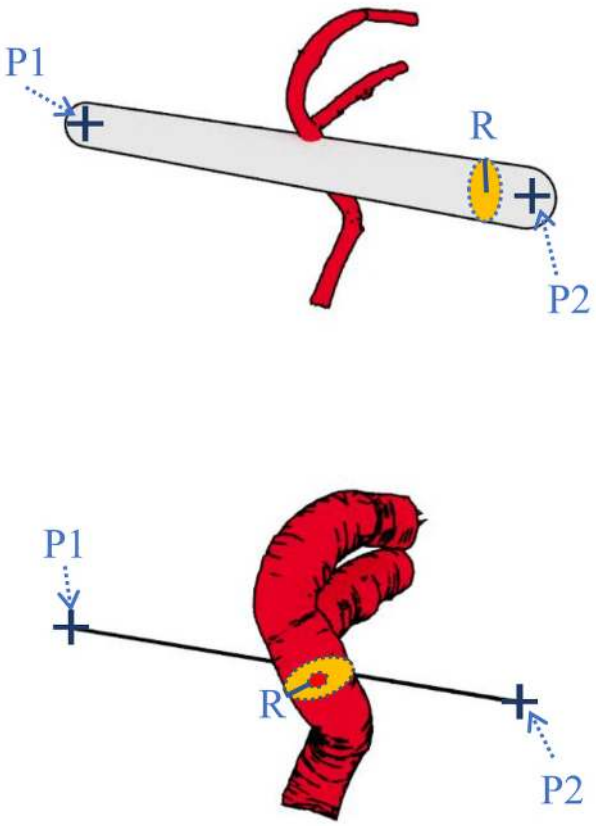

FIGURE 2. Computing if a path's security zone (defined by a capsule) hits the vessel (above) is equivalent to computing if the line segment P1P2 hits the enlarged vessels (below).

$$P_n = P_0 + RD \cdot n \cdot e^{i \cdot \omega \cdot n} \tag{2}$$

With:

$$\begin{aligned} n &= 0, 1, 2, ..., n_{max} \\ P_0, P_n &\in \mathbb{C} \end{aligned} \tag{3}$$

Where:

$$\begin{aligned} max(|\Delta P|) &= |P_n - P_0| \\ &= \left| RD \cdot n_{max} \cdot e^{i \cdot \omega \cdot n_{max}} \right| \\ &= RD \cdot n_{max} \end{aligned} \tag{4}$$

A new set of trajectories are evaluated for each iteration, and the search stops as soon as one avascular trajectory is found, or a maximum number of iterations ($n_{max} = 32$) is reached. The similar entry points lie on an Archimedean spiral (Fig. 5) and are visited in order (from the inside to

This article has been accepted for publication in a future issue of this journal, but has not been fully edited. Content may change prior to final publication. Citation information: DOI 10.1109/ACCESS.2021.3099964, IEEE Access

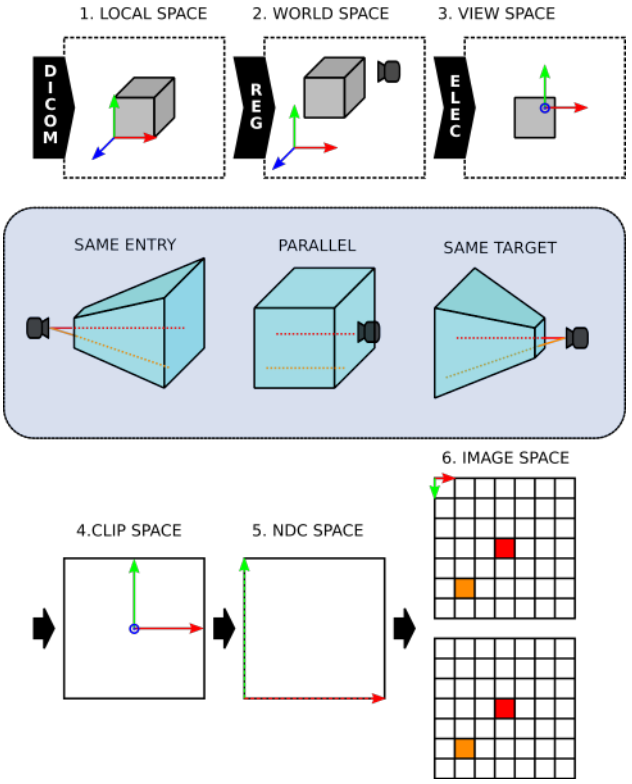

FIGURE 3. Graphical pipeline parametrized to compute electrode trajectories. In 3 different setups, 2 line segments (red and orange) are projected by different frustums, yielding the same final 2D image in viewport space. In all three cases, each trajectory gets collapsed into points/pixels.

the outside), with higher density near the initially selected entry (Fig. 6). The similar target strategy provides equal functionality but moving the target instead.

When more than one mask volume or mesh is available (e.g., DSA volumes for arteries or veins considered separately), each dataset is projected individually, and the resulting depth images are aggregated before the closest risk-free trajectory selection. The same approach is used when considering different SZ requirements along the length of the trajectory. This situation is depicted in Fig. 5, where two frustums (an orange frustum for the entry region and a black frustum for the rest of the electrode) are used to search for vessels at different subsections of the trajectory.

C. GUI: INTEGRATION WITH A SURGICAL PLANNER

The method has been integrated into SYLVIUS, a SEEG surgical planning system designed specifically for epilepsy surgery [34]. The DepthMap tool is controlled by the user with the interface depicted in Fig. 7. Here, information obtained from a DSA acquisition is used to provide the vascular structures. For each trajectory, the interface lists the avascular SZ diameter (i.e., twice the radial distance to the axis). The interface also signals collision with other SZ, which is computed by projecting the meshes of every other trajectory (green screen when no collisions, greyscale otherwise).

When the user clicks on any vessel on the DSA image seen

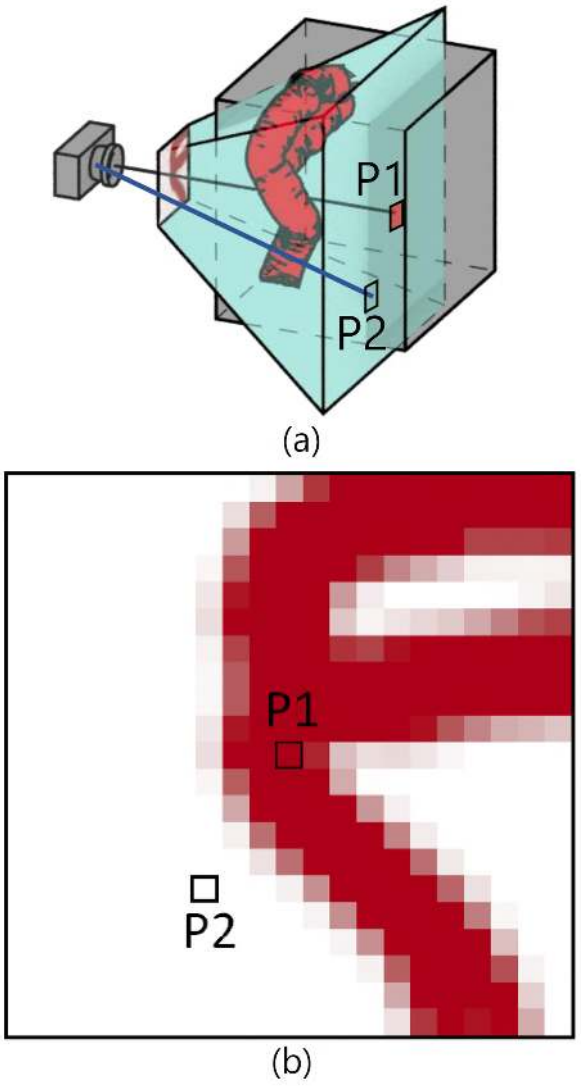

FIGURE 4. Above (a), a 3D distance map is rendered with a perspective frustum. Below (b), the final rendered image. P1 depicts the central pixel (which signals vessels inside the initial security zone) and P2 depicts one possible avascular path.

along the trajectory of the electrode, the 3D and tri-planar views get centered at that point for user inspection. For that, the transformations described in the previous section must be computed in reverse order, starting from the 2D image coordinates and its corresponding z-value, all the way back to world space. Please note that this requires the depth value, which is normally lost in normal rendering and MIP.

If a trajectory is found to be unsafe with the DepthMap tool, the AlternativeFinder tool can be configured with different avascularity requirements for the entry region (first 6 millimeters) and the rest of the trajectory. It can also be instructed to search for alternatives with a specific adherence strategy. When a trajectory is selected, only close by vessels are depicted in the 3D view to facilitate visual inspection.

This article has been accepted for publication in a future issue of this journal, but has not been fully edited. Content may change prior to final publication. Citation information: DOI 10.1109/ACCESS.2021.3099964, IEEE Access

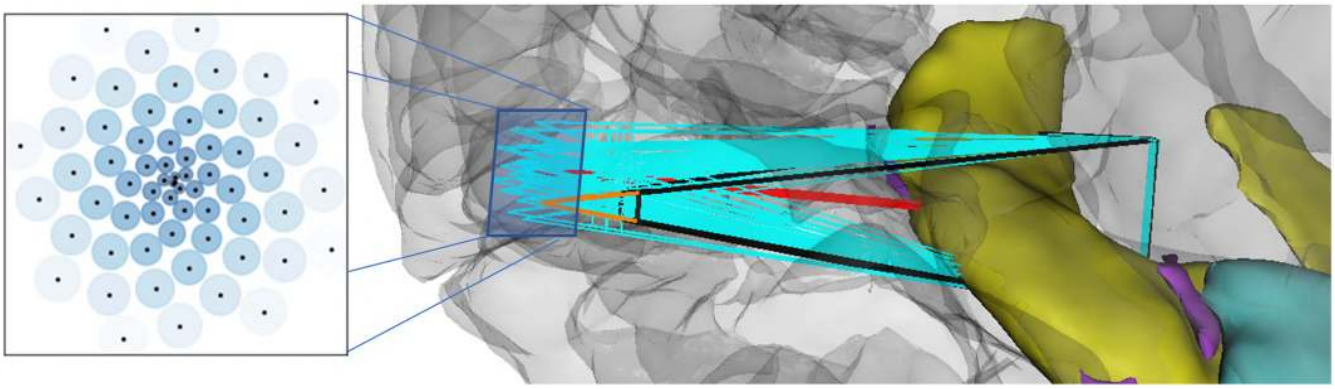

FIGURE 5. Spiral pattern for modifying the entry or target point (black dots) in the similar entry/target strategies. Each new point is 1 RD further away from P0 than the previous one, rotated another 135.5º, resulting in a bigger density towards the center. Two frustums (orange and black) are used to examine each subset of trajectories. The smaller orange frustum shows the one used for the computation of the entry-SZ constraint (7 mm), while the black one is the one used for the general SZ (5 mm) requirement. The preliminary trajectory is depicted in red.

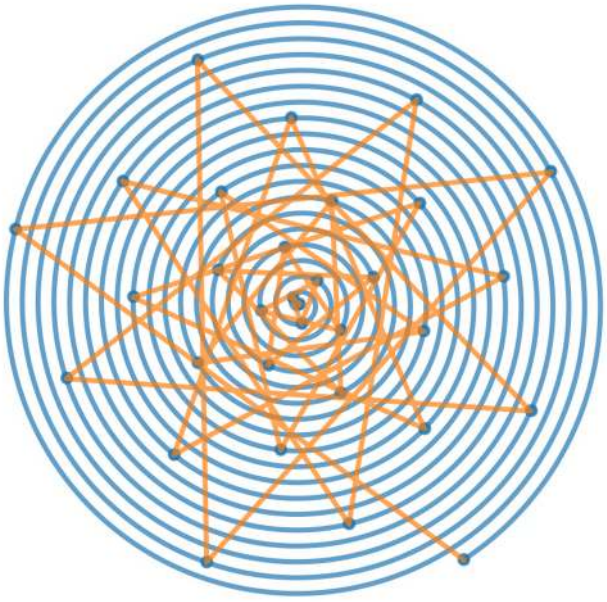

FIGURE 6. Similar entry/target alternative points (blue dots) placed over the Archimedean spiral (blue). A line is displayed to display the order in which points are traversed (yellow) until an avascular trajectory is found or a maximum number of iterations is reached.

D. EXPERIMENTAL DESIGN

To retrospectively evaluate both tools, a set of 12 patient cases requiring SEEG implantation was used. The study was approved by the local ethical committee on clinical investigations. All patients or their legal representatives provided written informed consent for the use of the data for research and publication. The cases were from Hospital del Mar, Barcelona (part of EpiCARE, the European Reference Network for epilepsy treatment) and contained preliminary and unrevised plans imported from two robotic platforms: the ROSA® (Zimmer Biomed Inc.) and neuromate® (Renishaw plc.). Electrode coordinates were imported referred to T1-weighted double-contrast Gadolinium T12c images (Philips Medical Systems, $256 \times 256 \times 100$ image resolution). The cases were then co-registered within SYLVIUS with their DSA datasets (Philips Medical Systems, $256 \times 256 \times 256$ resolution) and stored in a scene-graph data structure [34]. The registered DSA datasets (up to 4 for each case) were fused to produce a single 3D volumetric image. A threshold to segment vessels was then manually selected by a trained neurosurgeon, obtaining the vessel mask volume.

For each initial trajectory, the DepthMap tool was used to locate vessels inside the SZ. When vessels were found, Trajectory Finder was used to find alternatives. DepthMap was used once again to measure the alternative avascular diameter for comparison. The experiment was conducted on a laptop equipped with an Intel® Core™ i7-4810MQ CPU at 2.80GHz, and an NVIDIA Quadro K3100M GPU. Collision with other electrodes was not considered in the experiment.

The avascularity constraint was set to 7 mm in diameter for the first 6 mm of the trajectory (entry-SZ), and 5 mm diameter along the rest of the electrode. The number of electrodes that were already safe under that criteria, the ones with no alternative found, and the ones with alternative paths along with its type were recorded. To measure the adherence to the initial plan for each re-planning strategy, the Euclidean distance from the original and alternative entry and target points was computed. The re-planning computation time was also recorded for each trajectory and adherence strategy.

III. RESULTS

The alternative trajectories obtained following the described experimental design are shown in Fig. 8, arranged by the re-planning strategy used. For each alternative found, the avascular diameter measured for the initial (black) and the alternative (red, green, and blue) is shown, with an arrow connecting them. Distance to vessels is expressed as an equivalent avascular SZ diameter (twice the radial distance) for compatibility with the SZ convention used in the ROSA® and neuromate® robotic planning software. A histogram with the Euclidean distance between original and alternative

This article has been accepted for publication in a future issue of this journal, but has not been fully edited. Content may change prior to final publication. Citation information: DOI 10.1109/ACCESS.2021.3099964, IEEE Access

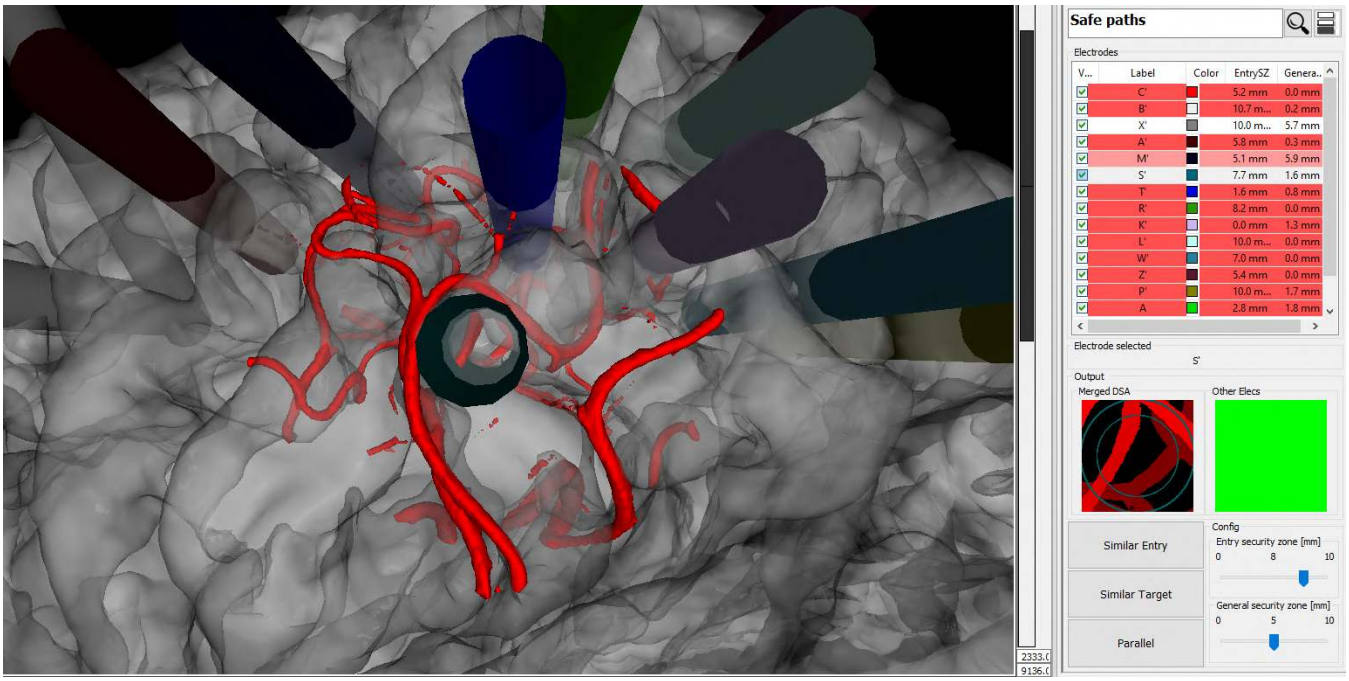

FIGURE 7. Left: 3D view with mask volume (i.e., DSA) only displayed around the selected electrode. Right top: entry and general SZ computed for each electrode. Right bottom: Selected electrode S' projected with a security zone of 8 mm in the entry and 5 in the rest. No other electrode in the trajectory is denoted by the green screen.

entry and target points is displayed for each re-planning strategy.

When an alternative was found, the average computation time was 77 ms per trajectory, with 75% of cases under 85 ms, and a maximum computation time of 765 ms. When no alternative was found, the time ranged between 8 and 889 ms. The average number of trajectories computed per millisecond was 1781 (with a central 50% of 1638-2028). Information regarding the total number of electrodes found in each case, its type, and computation times can be found in Table 1.

To evaluate a different use-case, an additional experiment was conducted aimed at maximizing distance-to-vessels. For each electrode, both the SZ and entry-SZ were measured with DepthMap, and later, the AlternativeFinder was run iteratively with increasing diameter of entry-SZ and SZ requirements (in steps of 1mm, favoring the entry-SZ over the SZ), until a maximum was found. Please note that when the diameter of the SZ is over 10 mm, it is presented as 10 mm in the graph, as that is the maximum diameter that can be measured with the DepthMap in the described configuration. In this additional experiment, every trajectory obtained enhanced avascular SZ values (Fig. 9).

IV. DISCUSSION

SEEG is a complex procedure requiring collaboration from several clinical specialties. The presented work fits in the workflow right after the epileptologist has provided its initial trajectories, and it is aimed at aiding neurosurgeons, with tools to early detect and discard problematic trajectories and find alternative ones when required. The AlternativeFinder tool is designed to adhere to different aspects of an initially planned trajectory. The reason we have not yet addressed the definition of that initial trajectory is that we have not found a practical way to that map seizure semiology (an important criterion for establishing the EZ localization hypothesis) into 3D space due to its non-image nature and complex symptom classification.

An experiment was presented to evaluate the search for the closest avascular trajectory given two fixed expected SZ values (usually the same for the whole plan). In the experiment, the user clicks and waits for the answer. Computation time is within acceptable values for an interactive tool, with response times well below one second. The presented method uses only hard constraints [11], [25], and it can early abort a search when no possible alternatives are found for one of the constraints (e.g., vessels at the entry), yielding response times as low as 8 ms for the parallel-alternatives computation.

As shown in Fig. 8, the similar entry approach produces smaller displacements on the entry than on the target. The opposite happens in the similar-target approach, demonstrating adherence to the initial trajectory in different ways. From all cited research, only De Momi *et al.* [11] addressed the issue of adherence to the entry and the target points and provides a qualitative evaluation of the results. Our study introduces a quantitative evaluation of the adherence adding yet another adherence option with the parallel strategy, obtaining alternative trajectories with the same insertion angles.

In Fig. 7 the histogram for parallel alternatives is identical for the entry and target point displacement, which was expected. This method may be used for parallel implantations

This article has been accepted for publication in a future issue of this journal, but has not been fully edited. Content may change prior to final publication. Citation information: DOI 10.1109/ACCESS.2021.3099964, IEEE Access

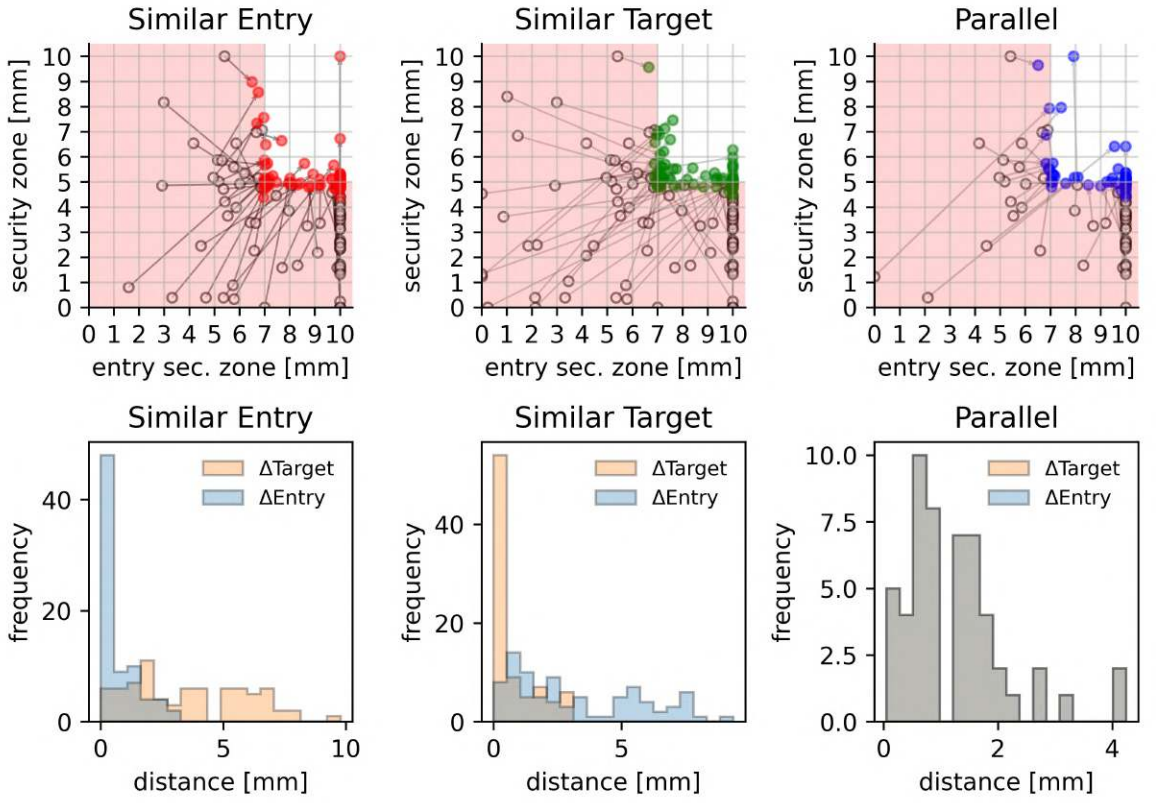

FIGURE 8. Above: Diameter of the trajectory security zones for original trajectory (empty white circle), and after the computation (red, green, and blue circles). A white square on the upper right corner depicts the area with acceptable SZ values. Below: histogram of the Euclidean distance between the original and safe path, for the target (red) and entry (blue) points.

TABLE 1. Trajectories studied with preliminary plans, detailing the type of alternative found, computation time, and the total number of alternatives computed (7mm entry sec. zone, 5mm sec. zone

				Alternative type			Computation	
Case	Electrodes	Already safe	With alternatives	Sim. Entry	Sim. Target	Parallel	Paths evaluated	Time [ms]
#1	10	1	8	7	7	5	8290304	4240
#2	14	7	7	7	7	7	2555904	1483
#3	8	4	4	4	4	4	1064960	750
#4	9	1	7	5	7	5	5783552	3160
#5	9	4	3	3	3	2	7700480	4120
#6	10	0	6	6	5	4	15843328	9900
#7	11	0	5	3	5	3	11714560	5907
#8	18	5	12	7	12	4	11288576	7028
#9	16	2	9	8	8	2	19791872	10188
#10	11	2	9	9	8	5	5701632	3296
#11	19	1	14	13	14	10	15056896	7821
#12	10	0	6	5	5	2	14090240	7214
Total	145	27	90	77	85	53	118882304	65107

This article has been accepted for publication in a future issue of this journal, but has not been fully edited. Content may change prior to final publication. Citation information: DOI 10.1109/ACCESS.2021.3099964, IEEE Access

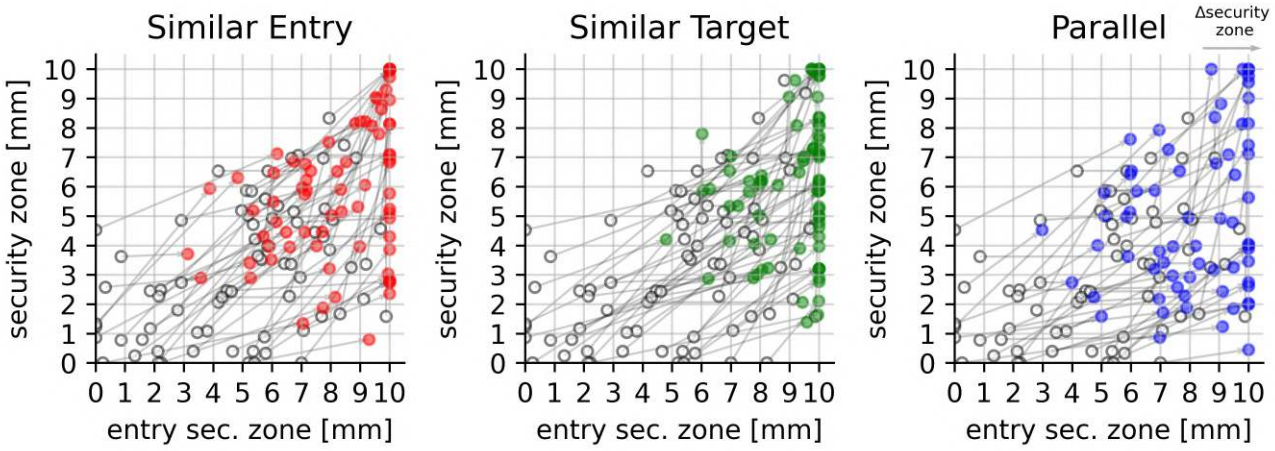

FIGURE 9. Dynamic optimization of entry-SZ and SZ. Every trajectory is enhanced in terms of an increase of its security zones, with a preference for the entry-SZ over the SZ. Preliminary trajectory security zones (empty white circle) are united to their final optimized trajectories (color depending on optimization strategy) with an arrow.

[32], [38], and it offers similarities with the original SEEG carried out in the Sainte Anne Hospital, France [4]. The parallel search described in this work is too strict and does not consider trajectories whose angles deviate slightly that of the initial trajectory, and it will be the subject of future work.

Visualization of surgical risk in a cortical mesh is valid for procedures where only the tip of the trajectory is relevant (e.g., DBS, needle biopsy) but it would not be useful for plotting risks associated with a fixed entry and multiple target points. Our visualization shares similarities with the MIP approach presented by the Milan group [24], but offers some extra advantages. The DepthMap tool records depth along the trajectory which is used by the user interface to let the user interactively inspect the tri-planar view of the original image simply by clicking on the desired part of the 3D vessel. This visualization is more natural to the user's eye than MIP, as objects closer to the user's eye occlude distant ones. Lastly, our tool scans the whole length of the trajectory, instead of the first centimeter. Our visualization provides radial positioning of the risks with respect to the trajectory axis, which cannot be visualized in the distance graph widget provided within Epinav [20]. This in turn provides more precise depth information that could be very useful during the implantation. Both visualization widgets are complementary and will be the subject of future work.

A recent publication examines 8 different heuristics used by different tools to optimize SEEG [39], where the first one was the maximizing distance from the vasculature. The second one was to avoid sulci (which we have tested using sulci information provided by Freesurfer [40]) but the main reason to do so is to avoid vessels, and we have opted to use DSA for that constraint. Furthermore, sulci avoidance conflicts with the next listed heuristic which is to maximize gray matter sampling. The drilling angle with the skull is another common heuristic, which our tool handles differently. Instead of providing the system with only a target point, we require an initial trajectory to be specified, and we guarantee that the trajectory does not deviate more than a certain angle.

The presented computations have the advantage of working directly with the original volumes, not requiring an intermediate mesh representation of the patient, although currently still require manual thresholding of the DSA. It can also be used with meshes, either with a distance map computation or directly projecting the mesh, in which case special care needs to be taken to prevent rendering of the inside of the mesh, which is empty and could return false negatives.

Another contribution of our method is that it is fully parametrizable, independently of the characteristics of the input datasets (e.g., cortical mesh resolution). This allows flexible configuration (search angle, number of trajectories to scan) through modification of specific parts of the rendering pipeline, as described in the DepthMap and AlternativeFinder subsections. When considering DSA imaging, finding avascular trajectories becomes more challenging than with a T1-weighted MRI scan with gadolinium enhancement, due to the increased number of vessels. DSA is an invasive technique with its own associated risks, and its benefits are under active investigation [41]. As discussed , visualization and assisted planning are highly dependent on vessel segmentation quality [23], which is an area of active research [42].

A pilot study has been conducted with clinicians from Hospital del Mar to evaluate the use of the described methods in a prospective setup, showing that the tool might be useful for early risk assessment. The tool has proven useful in finding avascular trajectories both from preliminary trajectories and for more definitive ones, where the algorithm performs very subtle modifications to the trajectories. The most prevalent cause of false-positive alternatives has been incorrect vessel segmentation. Another undesired effect happened when the proposed alternative moved to a different brain gyrus. The described method has been integrated into the

SYLVIUS stereotactic surgical planning platform. A patent has been filed for the Trajectory Finder method that searches for alternative trajectories. Future work will concentrate on exploring better segmentation of the DSA and other less invasive imaging modalities, computing electrode reports on tissue traversed, enhancing visualization and interaction, and providing preset avascular trajectory search within a certain brain region obtained from brain parcellations.

V. CONCLUSION

We have presented two automated tools that allow clinicians to examine and re-plan SEEG trajectories for avoiding risky structures while maximizing adherence with three possible adherence strategies, both performing at interactive speeds. A quantitative experiment has been conducted to measure the different re-planning strategies yield the expected adherence results. A graphical interface designed for trajectory evaluation in the clinical environment was implemented to allow the user to evaluate the tools. The presented tools work directly with volumetric images and can also be used with meshes. These tools provide early alarms and fast suggestions but do not replace the manual inspection of the trajectories, as they rely on the quality of the segmentation.

REFERENCES

[1] Patrick Kwan and Martin J. Brodie. Early Identification of Refractory Epilepsy. New England Journal of Medicine, 342(5):314–319, 2002.

[2] Takeharu Kunieda, Takayuki Kikuchi, and Susumu Miyamoto. Epilepsy surgery: surgical aspects. Current opinion in anaesthesiology, 25(5):533–9, oct 2012.

[3] Jorge Gonzalez-Martinez, Jeffrey Mullin, Sumeet Vadera, Juan Bulacio, Gwyneth Hughes, Stephen Jones, Rei Enatsu, and Imad Najm. Stereotactic placement of depth electrodes in medically intractable epilepsy. Journal of neurosurgery, 120(3):639–44, 2014.

[4] Francesco Cardinale, Giuseppe Casaceli, Fabio Raneri, Jonathan Miller, and Giorgio Lo Russo. Implantation of Stereoelectroencephalography Electrodes: A Systematic Review. Journal of Clinical Neurophysiology, 33(6):490–502, 2016.

[5] Francesco Cardinale, Massimo Cossu, Laura Castana, Giuseppe Casaceli, Marco Paolo Schiariti, Anna Miserocchi, Dalila Fuschillo, Alessio Moscato, Chiara Caborni, Gabriele Arnulfo, and Giorgio Lo Russo. Stereoelectroencephalography: Surgical methodology, safety, and stereotactic application accuracy in 500 procedures. Neurosurgery, 72(3):353–366, 2013.

[6] Jeffrey P. Mullin, Michael Shriver, Soha Alomar, Imad Najm, Juan Bulacio, Patrick Chauvel, and Jorge Gonzalez-Martinez. Is SEEG safe? A systematic review and meta-analysis of stereo-electroencephalography-related complications. Epilepsia, 57(3):386–401, 2016.

[7] Soha Alomar, Jaes Jones, Andres Maldonado, and Jorge Gonzalez-Martinez. The Stereo-Electroencephalography Methodology. Neurosurgery Clinics of North America, 27(1):83–95, 2016.

[8] Francesco Cardinale, Jorge González-Martínez, and Giorgio Lo Russo. SEEG, Happy Anniversary! World Neurosurgery, 85:1–2, 2016.

[9] Jean Isnard, Delphine Taussig, Fabrice Bartolomei, Pierre Bourdillon, Hélène Catenoix, Francine Chassoux, Mathilde Chipaux, Stéphane Clémenceau, Sophie Colnat-Coulbois, Marie Denuelle, Stéphane Derrey, Bertrand Devaux, Georg Dorfmüller, Vianney Gilard, Marc Guenot, Anne Sophie Job-Chapron, Elisabeth Landré, Axel Lebas, Louis Maillard, Aileen McGonigal, Lorella Minotti, Alexandra Montavont, Vincent Navarro, Anca Nica, Nicolas Reyns, Julia Scholly, Jean Christophe Sol, William Szurhaj, Agnès Trebuchon, Louise Tyvaert, Maria Paola Valenti-Hirsch, Luc Valton, Jean Pierre Vignal, and Paul Sauleau. French guidelines on stereoelectroencephalography (SEEG). Neurophysiologie Clinique, 48(1):5–13, 2018.

[10] Ignacio Delgado-martínez, Rodrigo Rocamora, Gerardo Conesa, and Luis Serra. Multidisciplinary planning of deep electrode implantation. In Gordon H. Baltuch and Arthur Cukiert, editors, Operative Techniques In Epilepsy Surgery, chapter Collaborat, pages 1–14. Thieme, 2nd editio edition, 2019.

[11] E. De Momi, C. Caborni, F. Cardinale, G. Casaceli, L. Castana, M. Cossu, R. Mai, F. Gozzo, S. Francione, L. Tassi, G. Lo Russo, L. Antiga, and G. Ferrigno. Multi-trajectories automatic planner for StereoElectroEncephaloGraphy (SEEG). International Journal of Computer Assisted Radiology and Surgery, 9(6):1087–1097, 2014.

[12] Mark Nowell, Roman Rodionov, Gergely Zombori, Rachel Sparks, Michele Rizzi, Sebastien Ourselin, Anna Miserocchi, Andrew McEvoy, and John Duncan. A Pipeline for 3D Multimodality Image Integration and Computer-assisted Planning in Epilepsy Surgery. Journal of Visualized Experiments, (111):53657, 2016.

[13] Mark Nowell, Roman Rodionov, Gergely Zombori, Rachel Sparks, Gavin Winston, Jane Kinghorn, Beate Diehl, Tim Wehner, Anna Miserocchi, Andrew W. McEvoy, Sebastien Ourselin, and John Duncan. Utility of 3D multimodality imaging in the implantation of intracranial electrodes in epilepsy. Epilepsia, 56(3):403–413, 2015.

[14] Charles A. Sansur, Robert C. Frysinger, Nader Pouratian, Kai Ming Fu, Markus Bittl, Rod J. Oskouian, Edward R. Laws, and W. Jeffrey Elias. Incidence of symptomatic hemorrhage after stereotactic electrode placement. Journal of Neurosurgery, 107(5):998–1003, 2007.

[15] Davide Scorza, Elena De Momi, Lisa Plaino, Gaetano Amoroso, Gabriele Arnulfo, Massimo Narizzano, Luis Kabongo, and Francesco Cardinale. Retrospective evaluation and SEEG trajectory analysis for interactive multi-trajectory planner assistant. International Journal of Computer Assisted Radiology and Surgery, 12(10):1727–1738, 2017.

[16] Yulong Zhao, Caroline Essert, Olga Dergachyova, Claire Haegelen, and Pierre Jannin. Automatic preoperative planning of DBS electrode placement using anatomo-clinical atlases and volume of tissue activated. International Journal of Computer Assisted Radiology and Surgery, 13(7):1117–1128, 2018.

[17] P. C. Herghelegiu, V. Manta, R. Perin, S. Bruckner, and E. Gröller. Biopsy Planner - Visual Analysis for Needle Pathway Planning in Deep Seated Brain Tumor Biopsy. Computer Graphics Forum, 31(3pt2):1085–1094, 2012.

[18] Esia Belbachir, Ehsan Golkar, Bernard Bayle, and Caroline Essert. Automatic planning of needle placement for robot-assisted percutaneous procedures. International Journal of Computer Assisted Radiology and Surgery, 13(9):1429–1438, 2018.

[19] Chiara Caborni, Elena De Momi, Luca Antiga, Abed Hammoud, Giancarlo Ferrigno, and Francesco Cardinale. Automatic trajectory planning in Stereo-electroencephalography image guided neurosurgery. International journal of computer assisted radiology and surgery, 7(Suppl 1):S126–S127, 2012.

[20] G. Zombori, R. Rodionov, M. Nowell, M. A. Zuluaga, Matthew J. Clarkson, C. Micallef, B. Diehl, T. Wehner, A. Miserochi, Andrew W. McEvoy, John S. Duncan, and Sśbastien Ourselin. A computer assisted planning system for the placement of sEEG electrodes in the treatment of epilepsy. In: Stoyanov D., Collins D.L., Sakuma I., Abolmaesumi P., Jannin P. (eds) Information Processing in Computer-Assisted Interventions. IPCAI 2014. Lecture Notes in Computer Science., 8498:118–127, 2014.

[21] Mario Rincon-Nigro, Nikhil V. Navkar, Nikolaos V. Tsekos, and Zhigang Deng. GPU-accelerated interactive visualization and planning of neurosurgical interventions. IEEE Computer Graphics and Applications, 34(1):22–31, 2014.

[22] M. Trope, R. R. Shamir, L. Joskowicz, Z. Medress, G. Rosenthal, A. Mayer, N. Levin, A. Bick, and Y. Shoshan. The role of automatic computer-aided surgical trajectory planning in improving the expected safety of stereotactic neurosurgery. International Journal of Computer Assisted Radiology and Surgery, 10(7):1127–1140, 2014.

[23] E. De Momi, C. Caborni, F. Cardinale, L. Castana, G. Casaceli, M. Cossu, L. Antiga, and G. Ferrigno. Automatic Trajectory Planner for StereoElectroEncephaloGraphy Procedures: A Retrospective Study. IEEE Transactions on Biomedical Engineering, 60(4):986–993, 2013.

[24] Davide Scorza, Sara Moccia, Giuseppe De Luca, Lisa Plaino, Francesco Cardinale, Leonardo S Mattos, Luis Kabongo, and Elena De Momi. Safe electrode trajectory planning in SEEG via MIP-based vessel segmentation. Proc. SPIE 10135, Medical Imaging 2017: Image-Guided Procedures, Robotic Interventions, and Modeling, 10135(i):101352C–101352C8, 2017.

[25] Rachel Sparks, Gergely Zombori, Roman Rodionov, Mark Nowell, Sjoerd B. Vos, Maria A. Zuluaga, Beate Diehl, Tim Wehner, Anna Miserocchi, Andrew W. McEvoy, John S. Duncan, and Sebastien Ourselin. Auto-

mated multiple trajectory planning algorithm for the placement of stereo-electroencephalography (SEEG) electrodes in epilepsy treatment. International Journal of Computer Assisted Radiology and Surgery, 12(1):123–136, 2017.

[26] Caroline Essert, Sara Fernandez-Vidal, Antonio Capobianco, Claire Haegelen, Carine Karachi, Eric Bardinet, Maud Marchal, and Pierre Jannin. Statistical study of parameters for deep brain stimulation automatic preoperative planning of electrodes trajectories. International Journal of Computer Assisted Radiology and Surgery, 10(12):1973–1983, 2015.

[27] Nikhil V. Navkar, Nikolaos V. Tsekos, Jason R. Stafford, Jeffrey S. Weinberg, and Zhigang Deng. Visualization and planning of neurosurgical interventions with straight access. Lecture Notes in Computer Science (including subseries Lecture Notes in Artificial Intelligence and Lecture Notes in Bioinformatics), 6135 LNCS:1–11, 2010.

[28] Reuben R. Shamir, Martin Horn, Tobias Blum, Janh Mehrkens, Yigal Shoshan, Leo Joskowicz, and Nassir Navab. Trajectory planning with augmented reality for improved risk assessment in image-guided keyhole neurosurgery. IEEE International Symposium on Biomedical Imaging: From Nano to Macro, pages 1873–1876, 2011.

[29] Alejandro De León-Cuevas, Saúl Tovar-Arriaga, Arturo González-Gutiérrez, and Marco Antonio Aceves-Fernández. Risk map generation for keyhole neurosurgery using fuzzy logic for trajectory evaluation. Neurocomputing, 233(August 2016):81–89, 2017.

[30] R. Zelmann, S. Beriault, M. M. Marinho, K. Mok, J. A. Hall, N. Guizard, C. Haegelen, A. Olivier, G. B. Pike, and D. L. Collins. Improving recorded volume in mesial temporal lobe by optimizing stereotactic intracranial electrode implantation planning. International Journal of Computer Assisted Radiology and Surgery, 10(10):1599–1615, 2015.

[31] Chiara Pastori, Stefano Francione, Federica Pelle, Marco de Curtis, and Vadym Gnatkovsky. Fluency tasks generate beta-gamma activity in language-related cortical areas of patients during stereo-EEG monitoring. Brain and Language, 163:50–56, 2016.

[32] Charles Munyon, Jennifer Sweet, Hans Luders, Samden Lhatoo, and Jonathan Miller. The 3-Dimensional Grid: A Novel Approach to Stereoelectroencephalography. Operative Neurosurgery, 11(1):127–134, mar 2015.

[33] Simon Drouin, Anna Kochanowska, Marta Kersten-Oertel, Ian J. Gerard, Rina Zelmann, Dante De Nigris, Silvain Bériault, Tal Arbel, Denis Sirhan, Abbas F. Sadikot, Jeffery A. Hall, David S. Sinclair, Kevin Petrecca, Rolando F. DelMaestro, and D. Louis Collins. IBIS: an OR ready open-source platform for image-guided neurosurgery. International Journal of Computer Assisted Radiology and Surgery, 12(3):363–378, 2017.

[34] Alfredo Higueras-Esteban, Ignacio Delgado-Martínez, Laura Serrano, Alessandro Principe, Carmen Pérez Enriquez, Miguel Angel González Ballester, Rodrigo Rocamora, Gerardo Conesa, and Luis Serra. SYLVIUS: A multimodal and multidisciplinary platform for epilepsy surgery. Computer Methods and Programs in Biomedicine, 203:106042, 2021.

[35] Alfredo Higueras-Esteban, Ignacio Delgado-Martínez, Laura Serrano, Gerardo Conesa, Miguel Angel González Ballester, and Luis Serra. Volume rendering depth mapping for fast vessel identification during intracranial deep electrode planning. International journal of computer assisted radiology and surgery (Suppl 1), 14(June):150–151, 2019.

[36] Will Schroeder, Ken Martin, and Bill Lorensen. The Visualization Toolkit. Kitware, Inc, 4th ed. edition, 2006.

[37] C R Maurer, Rensheng Qi, and V Raghavan. A linear time algorithm for computing exact Euclidean distance transforms of binary images in arbitrary dimensions. IEEE Transactions on Pattern Analysis and Machine Intelligence, 25(2):265–270, feb 2003.

[38] S. Medina Villalon, R. Paz, N. Roehri, S. Lagarde, F. Pizzo, B. Colombet, F. Bartolomei, R. Carron, and C. G. Bénar. EpiTools, A software suite for presurgical brain mapping in epilepsy: Intracerebral EEG. Journal of Neuroscience Methods, 303:7–15, 2018.

[39] Vejay N. Vakharia and John S. Duncan. Automation Advances in Stereoelectroencephalography Planning. Neurosurgery Clinics of North America, 31(3):407–419, 2020.

[40] Bruce Fischl. FreeSurfer. NeuroImage, 62(2):774–781, 2012.

[41] Ignacio Delgado-Martínez, Laura Serrano, Alfredo Higueras-Esteban, Elio Vivas, Rodrigo Rocamora, Miguel A. González Ballester, Luis Serra, and Gerardo Conesa. On the Use of Digital Subtraction Angiography in Stereoelectroencephalography Surgical Planning to Prevent Collisions with Vessels. World Neurosurgery, 147:47–56, 2021.

[42] Maria A. Zuluaga, Roman Rodionov, Mark Nowell, Sufyan Achhala, Gergely Zombori, Alex F. Mendelson, M. Jorge Cardoso, Anna Miserocchi, Andrew W. McEvoy, John S. Duncan, and Sébastien Ourselin. Stability, structure and scale: improvements in multi-modal vessel extraction for SEEG trajectory planning. International Journal of Computer Assisted Radiology and Surgery, 10(8):1227–1237, 2015.

ALFREDO HIGUERAS-ESTEBAN received his degree in Telecommunications Engineering from the Universidad Politécnica de Madrid, Spain, in 2008. He is currently pursuing a Ph.D. degree in information and communications technology from the Universitat Pompeu Fabra in Barcelona, Spain.

From 2008 to 2009 he worked as a Field Engineer at ASSYCE, Granada, Spain, developing supervisory control and data acquisition systems for industrial solar power plants. From 2010 to 2015 he was an Analyst at the Global Markets Risk Unit from BBVA, Madrid, Spain, writing software for the evaluation of commodities, equity, and interest rates securities. Since 2015 he is working at Galgo Medical, Barcelona, Spain, as a Software Engineer in the development of neurosurgical planning solutions. He is the author of two articles and holds one patent.

Mr. Alfredo Higueras-Esteban's research interests include surgical planning, programming, 3D interaction and graphical visualization.

IGNACIO DELGADO-MARTÍNEZ received a medical degree from the University of Cantabria, Spain, in 2002.

In 2006, he received the M.D., Ph.D. degree from the University of Göttingen, Germany for his thesis work in synaptic transmission at the Max-Planck Institute. In 2008, he joined the Department of Neurosurgery of the University Hospital Charité of Berlin, Germany, where where he underwent specialist neurosurgical training. Since 2014 he has been working on the SYLVIUS project together with the Neurosurgical Department of Hospital del Mar, Barcelona, and Galgo Medical.

M.D. Ph.D. Delgado-Martinez has authored over 30 peer-reviewed publications with more than 400 citations and several chapters in scientific textbooks. His interests include neurosurgical prosthetics and operative neurotechnology.

LAURA SERRANO PÉREZ received her degree in medicine from Universitat Autònoma de Barcelona (UAB) in 2010. From 2011 to 2016 she underwent specialist neurosurgical training at the Hospital del Mar, Barcelona. She has been an active member of the epilepsy unit since its inception. The Hospital del Mar Epilepsy Unit has been distinguished in Catalonia as a reference center for epilepsy surgery by CatSalut and by the Ministry of Health as a center National Reference for Refractory Epilepsy CSUR. At an international level, the Epilepsy Unit is part of the European project of the Epilepsy Surgery Center Network (E-pilepsy).

She has performed functional neurosurgery rotation at Grenoble Hospital (France), specifically in the fields of epilepsy surgery and deep brain stimulation. She has also performed a functional neurosurgery rotation at the National Hospital for Neurology and Neurosurgery, Queen Square (London), specifically in epilepsy surgery, and at San Joan de Deu Hospital in Barcelona and at Santobono Pausillon Hospital in Naples, in pediatric neurosurgery.

M.D. Serrano Pérez is a member of the Spanish Neurosurgical Society (SENEC).

NAZARET INFANTE SANTOS was born in Barcelona, Spain, in 1988. She received the M.D. degree in Medicine from the Universitat de Barcelona, in 2012.

From 2013 to 2018 she did her training in neurosurgery at Hospital Universitario Reina Sofía, in Córdoba, Spain. From 2018 to 2020, she worked as a Neurosurgeon Consultant in Neurosurgery Department at Córdoba, focusing on neurooncology and spinal pathologies. She obtained a master in bioinformatics and biostatistics in 2020, from the Universitat Oberta de Catalunya, and a master in neurooncology, from the Universidad CEU Cardenal Herrera, in Madrid. She recently moved to Barcelona, where she is working at Hospital del Mar, being part of the epilepsy group.

M.D. Infante Santos is a member of the Spanish Neurosurgical Society (SENEC). Her research interests include epilepsy surgery and neurooncology.

ALEJANDRA NARVÁEZ-MARTÍNEZ was born in Neiva, Huila, Colombia in 1983. She received the medical degree from the National University of Colombia, Bogotá, Colombia, in 2007 and the Ph.D. degree in Medicine from Universitat Autònoma de Barcelona, Catalonia, Spain, in 2018.

From 2011 to 2017 she underwent specialist neurosurgical training at Hospital Universitario de Girona Dr. Josep Trueta, Girona, Catalonia, Spain. Since 2018, she is a consultant neurosurgeon at Hospital del Mar, Barcelona, Catalonia, Spain. She is the author of 5 articles published in national and international journals. Her research interests include epilepsy and neuro-oncology.

M.D. Ph.D. Narváez-Martínez is a member of the Spanish Neurosurgical Society (SENEC) and the European Association of Neurosurgical Societies (EANS).

ALESSANDRO PRINCIPE is an Associate Physician, specialist in clinical neurophysiology of the Epilepsy Unit (UE) of the Hospital del Mar and collaborates with the neuroscience and neuropharmacology group of the Institut del Hospital del Mar d'Investigacions Mèdiques (IMIM).

In 2014 he was a Fellow in the Department of Epilepsy and Malaises Neurologiques of the University Hospital of Grenoble, France, where he collaborated in clinical-scientific projects under the guidance of Prof. Philippe Kahane. From 2010 to 2014 he worked as a Resident Physician in the specialty of clinical neurophysiology at the same hospital. From 2007 to 2010 he worked as a Doctor in the Department of Internal Medicine, Cardioangiology, and Hepatology at the University of Bologna.

M.D Ph.D. Principe obtained the title of doctor cum laude in applied physiology and pathophysiology in 2007, jointly with the University of Barcelona.

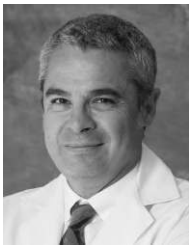

RODRIGO ROCAMORA is the Head of the Epilepsy Monitoring Unit of the Department of Neurology in Hospital del Mar and is currently Associated Professor of biomedical engineering at the Universitat Pompeu Fabra, Barcelona.

From 1999 to 2001 he was awarded by the German Government with the DAAD Scholarship at the Epilepsy Clinic in the University of Bonn. His research assessed the modulating effect of sleep over the epileptic activity in patients with temporal lobe epilepsy evaluated by invasive recordings. In 2011 he obtained his Ph.D. in medicine at the University of Bonn. Posteriorly, he worked as an Epileptologist at the universities of Marburg (2002-2004) and Freiburg (2004-2006). From 2007 to 2009 he was Director of the Sleep Centre at Hospital Ruber Internacional Madrid, Spain.

M.D. Ph.D. Rocamora is currently the Coordinator of the Epilepsy Surgery in Catalonia and a Spanish member of the scientific committee for epilepsy at the EAN (European Academy of Neurology).

GERARDO CONESA received his M.D. in 1982 at the University of Barcelona. He specialized in neurosurgery in 1990 in the Hospital of Bellvitge in Barcelona and got his Ph.D. in 1994 at the University of Barcelona. He has been Assistant Professor of neurosurgery since 2000 at the University of Barcelona and changed to the Autonomous University of Barcelona in 2012.

After residency program training, he has worked as Attending Neurosurgeon in the Hospital of Bellvitge until 2003, as Consultant Neurosurgeon in the Hospital Clinic of Barcelona until 2007, as Chief of neurosurgery in Hospital del Mar in Barcelona until 2018, and later on as Chief of neurosurgery in Hospital del Mar and Hospital de Sant Pau until 2020.

M.D. Ph.D. Conesa is now the Director of Teknon Neurosciences Institut in Barcelona and is responsible for the epilepsy surgery program in Hospital del Mar.

LUIS SERRA hails from Barcelona, Spain, and received a Ph.D. and MSc in electrical engineering in 1987 from the School of Information Technology Systems, University of Bradford (UK) and a degree in telecommunications engineering from the Universitat Politècnica de Catalunya in 1982.

From 1988 to 1999 he was a Member, Research Staff at the Institute of Systems Science in Singapore. There he developed the Dextroscope, a VR interface for the manipulation of 3D medical imaging data. In 2000 he co-founded Volume Interactions Pte Ltd, a Singapore spin-off company setup to commercialize the Dextroscope technology. Volume Interactions applied the Dextroscope technology to radiology and neurosurgery, creating products for pre-operative planning and image-guided surgery. The company was bought by the Bracco Group in 2002, had operations in Europe, China, and the USA. Back in Spain, he co-founded Galgo Medical SL (Barcelona) in 2013, a software company dedicated to providing 3D medical imaging surgical planning solutions.

Ph.D. Serra leads the development of the arrhythmia care and neurosurgery lines. He is the author of more than 20 articles, and more than 25 inventions. His research interests include surgical planning based on medical imaging, and virtual reality.

MIGUEL A. GONZÁLEZ BALLESTER (Senior Member, IEEE) holds a computer science degree from Universitat Jaume I, Spain (1996) and a doctoral degree from the University of Oxford, UK (2000).

He held senior researcher / faculty positions at Toshiba Medical Systems (Japan), INRIA (France) and the University of Bern (Switzerland). From 2008 until 2013 he led the Research Department of the company Alma IT Systems in Barcelona (Spain), and in 2013 he became ICREA Professor at the Department of Information and Communication Technologies of Universitat Pompeu Fabra (UPF) in Barcelona, Spain. He is director of the BCN Medtech research unit at UPF, and has more than 300 publications in peer-reviewed scientific journals and conferences. He was program chair of the IEEE International Symposium on Biomedical Imaging 2019.

Prof. González Ballester's research interests include image processing and computer vision for medical image analysis, computer assisted surgery and computational simulation for predictive medicine.